

ORIGINAL ARTICLE

Internal vascular channel architecture in human auditory ossicles

Shivani M. Manoharan¹ | Roger Gray¹ | John Hamilton² | Matthew J. Mason¹ 

¹Department of Physiology, Development & Neuroscience, University of Cambridge, Cambridge, UK

²Department of Otolaryngology, Gloucestershire Hospitals NHS Trust, Gloucester, UK

Correspondence

Matthew J. Mason, Department of Physiology, Development & Neuroscience, University of Cambridge, Cambridge CB2 3EG, UK.

Email: mjm68@cam.ac.uk

Abstract

The vascular supply of the human auditory ossicles has long been of anatomical and clinical interest. While the external blood supply has been well-described, there is only limited information available regarding the internal vascular architecture of the ossicles, and there has been little comparison of this between individuals. Based on high-resolution micro-CT scans, we made reconstructions of the internal vascular channels and cavities in 12 sets of ossicles from elderly donors. Despite considerable individual variation, a common basic pattern was identified. The presence of channels within the stapes footplate was confirmed. The long process of the incus and neck of the stapes showed signs of bony erosion in all specimens examined. More severe erosion was associated with interruption of some or all of the main internal vascular channels which normally pass down the incudal long process; internal excavation of the proximal process could interrupt vascular channels in ossicles which did not appear to be badly damaged from exterior inspection. An awareness of this possibility may be helpful for surgical procedures that compromise the mucosal blood supply. We also calculated ossicular densities, finding that the malleus tends to be denser than the incus. This is mainly due to a lower proportion of vascular channels and cavities within the malleus.

KEYWORDS

auditory ossicles, density, erosion, long process, middle ear, vascularization

1 | INTRODUCTION

The auditory ossicles play an essential role in sound transmission, and damage to them leads to conductive hearing loss. The predisposition of certain parts of the human ossicular chain to erosion is taken to be due to the pattern of blood supply, the long process of the incus being especially vulnerable (Gerlinger et al., 2009; Lindeman, 1964). Hamberger and Wersäll (1964) found that the internal channels in this process can be 'extremely thin,' especially where there had been previous infections, and linked a poor blood

supply to decalcification. Surgical techniques may also result in ossicular damage by compromising the blood supply (Alberti, 1963; Alberti, 1965; Enghag et al., 2019; Vallejo-Valdezate et al., 2016). Understanding the pattern of ossicular microvasculature of the ossicles is a first step towards being able to avoid such problems.

Early studies of the vascular architecture of the human auditory ossicles were based on histology and light microscopy. Nager and Nager (1953) examined in detail histological serial sections through 10 temporal bone specimens from five young adult individuals, and looked briefly at another 100 series. They found that an ossicular

This is an open access article under the terms of the [Creative Commons Attribution-NonCommercial](https://creativecommons.org/licenses/by-nc/4.0/) License, which permits use, distribution and reproduction in any medium, provided the original work is properly cited and is not used for commercial purposes.

© 2022 The Authors. Journal of Anatomy published by John Wiley & Sons Ltd on behalf of Anatomical Society.

branch of the anterior tympanic artery divides to form the malleolar and incudal arteries, which provide the main internal blood supply to the malleus and incus respectively. A network of vessels within the ossicular mucosa gives rise to very small branches which also penetrate the ossicles, joining the internal channel structure. This external, mucosal network is mainly supplied by the anterior tympanic artery, with some contribution from the stylomastoid and deep auricular arteries to the network around the manubrium. Within the stapes, blood vessels were only identified in the rim of the footplate and in the neck and head, the rest of the ossicle apparently being supplied only by diffusion from mucosal vessels. The mucosal network of the stapes is supplied by branches of the superficial petrosal, superior and inferior tympanic arteries. The architecture of the internal 'vascular convolute' of the ossicles was only briefly described, and not illustrated.

Hamberger et al. (1963) and Hamberger and Wersäll (1964) concentrated mainly on the mucosal supply of the ossicles. They briefly commented on the poor internal supply of the manubrium and incudal long process, and the absence of internal vascular channels in the crura and footplate of the normal stapes. Lindeman (1964) provided some photomicrographs of incudal and stapedia cross-sections, showing the vascular channels, and commented on the positions of the nutrient foramina.

Kirikae (1960) showed photomicrographs of the blood vessels within a cleared malleus and incus, and provided sketches of the positions of the main vessels. More detailed reconstructions of the internal vascular architecture of the three ossicles were made by Anson et al. (1964), based on serial histological sections taken from a neonate and three young adults. This was developed further by Anson and Winch (1974). These authors created their reconstructions from tracings made on cardboard sections. They show a very complex network of relatively wide vessels within the malleus and incus, with no clear pattern visible except for trends that were noted in the transverse or longitudinal orientations of the vessels, and the presence of wider channels centrally. The impression from their illustrations is of a tangle of vascular channels which would collectively occupy a high proportion of the total ossicular volume.

Following the early reconstructions by Kirikae and Anson's group, the internal vascular channels of the human ossicles have been reexamined using more modern methods. Bradel et al. (2017) compared the use of micro-CT and a micro-grinding histological technique. They provided reconstructions of the 'not calcified' internal structures of both malleus and incus, which included the vascular channels. Enghag et al. (2019) CT-scanned 20 temporal bones, and undertook synchrotron phase-contrast imaging on a further seven, focusing on the distal long process of the incus and associated structures. The highest-quality reconstructions of the internal architecture so far available come from Anschuetz et al. (2019), who looked at all three ossicles from three temporal bones using synchrotron phase-contrast imaging, and achieved sub-micron resolution for the first time.

Although Enghag et al. (2019) discussed individual variations in the vascular supply to the distal long process, the supply to the rest

of the ossicular chain has not been described in detail, and there has been little consideration of the main patterns and their variation between individuals. A better knowledge of this could help to progress our understanding of the pathology of the auditory ossicles, as well as informing surgical approaches. To this end, we produced high-resolution micro-CT reconstructions of the internal vascular architecture in 12 sets of human auditory ossicles, from elderly donors. We identify and illustrate the basic pattern of main channels, and describe the considerable variation found between the ossicles of the individuals examined. This variation was based on differences in channel density and pattern, and erosion of parts of the ossicular chain.

Ossicular masses and densities are parameters important to the modelling of middle ear function (e.g. Hemilä et al., 1995; Homma et al., 2009; Sim et al., 2007; Zhou et al., 2019). We compared these values in our 12 specimens, and provide a brief commentary on how density differences between the malleus and incus relate to the channels and cavities within.

2 | MATERIAL AND METHODS

Twelve human temporal bone specimens were obtained from the Human Anatomy Centre in the Department of Physiology, Development & Neuroscience, University of Cambridge. These came from four male and eight female donors, aged between 70 and 98 years. The male temporal bones included two left and two right specimens; the female temporal bones included four left and four right specimens. Only one temporal bone was used per donor. Prior to decease, all donors had given consent for the use of their bodies for anatomical research, in compliance with the Human Tissue Act 2004, but no detailed medical histories were provided. The donated bodies had been embalmed through cannulation of the common carotid or femoral arteries, and injection under pressure of a solution comprising 4.2% formaldehyde, 38% ethanol, 1.5% methanol and 56.3% water. The temporal bones had been cut down with a band-saw to rough cuboids which included the middle and inner ears, and had been CT-scanned as part of previous projects. No gross abnormalities of the middle ear were observed in these scans. The 12 temporal bones were then kept moist in sealed plastic bags, and refrigerated prior to their use in the current study. We dissected out the auditory ossicles from these temporal bones using standard dissection equipment plus a hand-held drill burr. The soft tissue attachments of the malleus and incus to the rest of the skull were severed, and the incudo-stapedial articulation was separated with a scalpel blade. The malleus and incus were then removed. The bone around the oval window was drilled away, to facilitate removal of the stapes after severing the stapedius tendon. Five stapedes were obtained intact in this way, the other seven suffering variable amounts of damage, usually to the footplate.

Following air-drying, the malleus, incus and stapes from each donor were placed on radio-translucent foam and CT-scanned together, at the highest magnifications possible, in a Nikon XT H 225

micro-CT scanner. Settings of 130kV and 130 μ A, with exposure time of 1000ms, were used for each of the 12 scans made. In total, 1080 projections were made in each case, with two frames averaged per projection. No filters were used. The scans were processed using CT Agent XT 3.1.9 and CT Pro 3D XT 3.1.9 (Nikon Metrology, 2004–2013), and 16-bit tiff stacks were created with cubic voxel side-lengths of 4.5–6.7 μ m. The windowing chosen was based on linear attenuation coefficients from 0 (air; black) to 150mm⁻¹ (white), for all scans. These values represented the narrowest window encompassing the attenuation range of air, soft tissue and ossicular bone, so as to maximise visible contrast. Adobe Photoshop CS 8.0 (Adobe Systems Inc., 2003) was then used to convert the tiffs to high-quality 8-bit jpg files, which were loaded into Stradview 6.13. Stradview, used to create 3D reconstructions, was written by Graham Treece & Andrew Gee of the Medical Imaging Research Group at the University of Cambridge.

Following a comparison of the tomograms, a threshold greyscale value was selected by eye, above which a voxel would be considered as 'bone' and below which it would be considered as 'non-bone' (i.e. air or soft tissue). In all 12 scans, this same threshold value was used within Stradview to identify the perimeter of each ossicle automatically, every eight frames. The perimeters selected in this way were outlined and then manually corrected, to separate the ossicles where they were touching and to remove from the reconstructions any stray fragments of bone clinging to the ossicles. Next, using the same threshold value, Stradview was used to outline the boundaries of the channels and cavities within the ossicles. These outlines were identified every four frames, for improved resolution.

We use the term 'channel' to mean a tube-like space within the ossicular bone, while 'cavity' refers to a more voluminous and less cylindrical space. While some of the larger channels and cavities appeared to be at least partially air-filled (black pixels in the tomograms), many of the smaller channels contained soft tissue (grey pixels). It was not possible to identify the soft tissue contents of these channels and cavities from tomograms. However, based on a comparison with many histological studies of the ossicles in the literature, these channels and cavities were interpreted as having contained blood vessels *in vivo*, and are hence described as 'vascular' (see Discussion section 'Contents of ossicular channels and cavities'). Although the wider channels and cavities likely contained more than one blood vessel and connective tissue too, only the outline of these spaces could be identified and reconstructed.

The smallest objects identifiable as channels in each tomogram were based on individual pixels that were darker than our chosen bone/non-bone greyscale threshold. Reconstruction of the smallest channels was, therefore, limited by our scan resolution and by our choice of threshold. We could see that some of the smaller channels containing soft tissue were not picked out by our automated selection process, but would have been had we chosen a lighter threshold. However, it was deemed important for reasons of comparability that we use the same threshold for all of our reconstructions, and changing the value so as to pick out more of the smaller channels would have expanded the apparent volume of the more significant

channels and cavities beyond what seemed reasonable from visual inspection. Because priority was given to these larger vacuities, our reconstructions do not show the smallest channels within the ossicular structure.

The ossicular perimeters included invaginations where vascular channels penetrated into the ossicular structure, whereas the internal boundaries were only for those channels and cavities with no contact with the surface. Subtracting the volume of these internal channels and cavities from total ossicular volume gave the volume of the ossicular bone only. In order to create better representations of the vascular architecture, however, the points where the channels reached the surface had to be included. The cut-off between each channel and the air surrounding the ossicle, at the ossicular surface, had to be estimated and drawn in manually in each case.

As described in the Results, we found what appeared to be significant erosion of the long process of the incus in particular in many of our specimens. What we interpreted as air-filled, eroded spaces were peripherally located, with some open connection to the exterior of the ossicle. They were often much more voluminous than the vascular channels in the same area, and were more irregular in outline (Figure 1). These regions proved difficult to reconstruct because

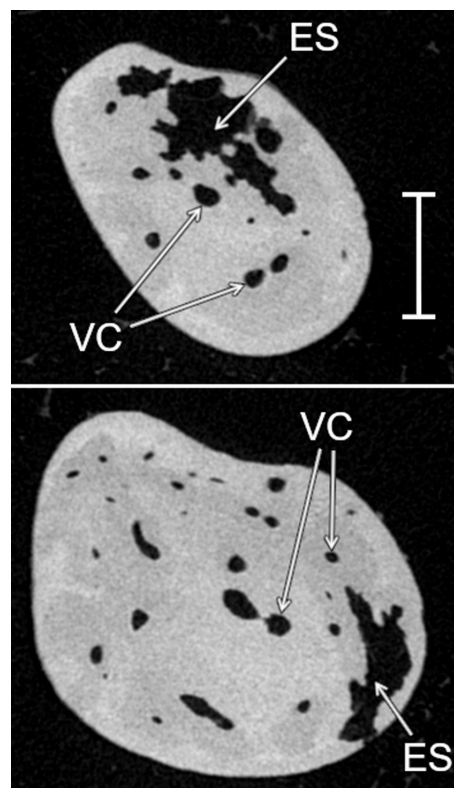


FIGURE 1 Tomogram cross-sections at two different positions through the long process of the same incus. Large vacuities identified as eroded spaces (ES) are peripherally located, and more irregular in outline than vascular channels (VC). The eroded region in the upper panel is not in communication with the exterior in this particular section, but it did open to the exterior elsewhere. Two vascular channels are indicated as examples in each tomogram, but many more are visible. Scale bar 0.5mm

vascular channels sometimes opened into the larger eroded cavities, and we had to use our best judgment to position the cut-off between the two.

The outlines of the ossicles and their internal channels and cavities were used to create 3D, rotatable images. Volumes were calculated automatically in Stradview, given the voxel size and the spacing between frames. The three volumes which were used in subsequent calculations were (1) ossicular bone volume, (2) intraossicular vascular channel/cavity volume and (3) total ossicular volume, which was the sum of (1) and (2). The percentage of internal channels and cavities was calculated from the vascular channel/cavity volume divided by total ossicular volume. The volumes of eroded spaces were not included in any of these measurements.

After scanning, the ossicles were weighed on a Cahn C-31 microbalance. Prior to weighing, the ossicles were cleaned as well as possible without risking damage, but there was still some dried soft tissue, for example shreds of ligaments, clinging to the specimens. Ossicular densities were calculated as these masses divided by the total ossicular volumes. Bone densities represent the mass of the osseous component only divided by ossicular bone volume, ignoring the channels and cavities within the ossicles. Because assumptions needed to be made about the masses used in the calculations, bone density calculations are described further in the Discussion.

Some of the reconstructions were laterally inverted to make all ossicles appear as right ossicles in the illustrations, for easier comparison.

The CT data that support the findings of this study are available on request from the corresponding author. The data are not publicly available due to privacy and ethical restrictions.

3 | RESULTS

The CT reconstructions made in this study were primarily used to establish the volume and architecture of the vascular channels and cavities within the ossicles. These channels and cavities formed a complicated, intercommunicating network, with branches reaching the surfaces of the ossicles via multiple foramina. Many of the smallest channels visible by eye in the tomograms were not identified in our reconstruction process (see Methods).

3.1 | Malleus

The most radiodense part of the malleus head was around the periphery; the interior of the head had the lowest radiodensity of any part of the ossicle (Figure 2a). The neck and manubrium tended to be very radiodense, the lateral and anterior processes intermediate.

The malleus contained a very complex network of branching and anastomosing channels. Although there was considerable individual variation between the specimens examined, it was possible to pick out a consistent basic pattern upon which these variations were superimposed, centring on a major channel running along the long axis of the malleus (Figure 2a). This axial channel extended downwards from an expanded cavity in the centre of the malleus head, ran ventrolaterally through the neck towards the lateral process, where it would usually send off a branch to the process itself, changing direction there to run ventromedially within the manubrium. Within the manubrium, the long, narrowing channel was located nearer to the lateral, inserting margin than to the medial margin, and it usually ran almost to the tip. In nine specimens, it branched somewhere within

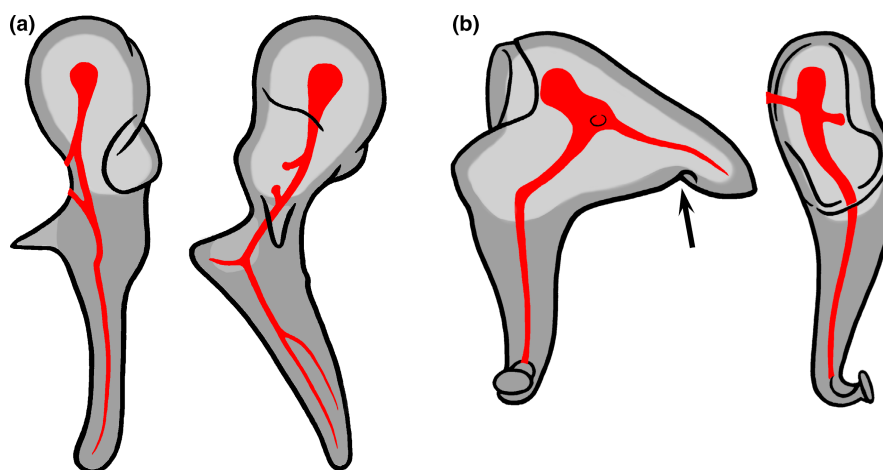


FIGURE 2 Diagrammatic representations of the typical patterns of the main vascular channels and cavities, shown in red, within (a) the malleus and (b) the incus. Right ossicles, each seen from (left) medial and (right) anterior views. In the malleus, two communicating channels connecting the main system to the exterior are shown, just dorsal to the anterior process. In the incus, communicating channels medial and lateral to the main cavity are shown. The channel extending down the long process has an exit-point just dorsal to the pedicle supporting the lenticular apophysis. The main channels in the longer processes are normally accompanied by several others running in parallel, and there are many other branching and anastomosing channels radiating out from the cavities in the heads of the ossicles, obscuring this basic architecture. These are not shown. The grey shading gives a broad indication of the typical patterns of radiodensity of the bony component of the ossicles; darker shading represents higher radiodensity. The arrow indicates the notch in the short process of the incus, observed in many specimens

the manubrium, generating a parallel branch running closer to the centre of that process.

In eight mallei, the major connections between the main axial channel and the exterior of the ossicle were through one or two larger foramina in the roughened area of bone dorsal to the anterior process, to which the axial channel was linked by short communicating channels. In another three specimens which had two large foramina dorsal to the anterior process, the main axial channel was interrupted. The upper foramen in these specimens sent a channel to the cavity within the malleus head, while the lower one sent a channel down through the neck to the manubrium. From what could be seen of the residual soft tissue, it seemed that a single vessel had forked prior to entering the bone, sending branches into two channels rather than one main channel. The last malleus also had a discontinuous axial channel, but this specimen, which had an unusually

sparse channel structure in both malleus and incus, lacked any major communicating foramina dorsal to the anterior process.

Within the head of the malleus, the central cavity ranged from a fairly capacious, lens-shaped or polygonal chamber to little more than an expanded channel. The largest channels would be those radiating off the central cavity: These varied a lot in size and density, and would branch and interconnect with others, obscuring the basic pattern (Figure 3). The channel density in the neck and manubrium of the malleus was lower than in the head. As well as the main axial channel described above, a variable number of other channels would run in parallel through the neck and manubrium. The larger channels would generally be aligned along the long axis of the ossicle, although there was a lot of intercommunication between them. Although there would always be multiple additional channels in the proximal manubrium and lateral process, the channels dwindled

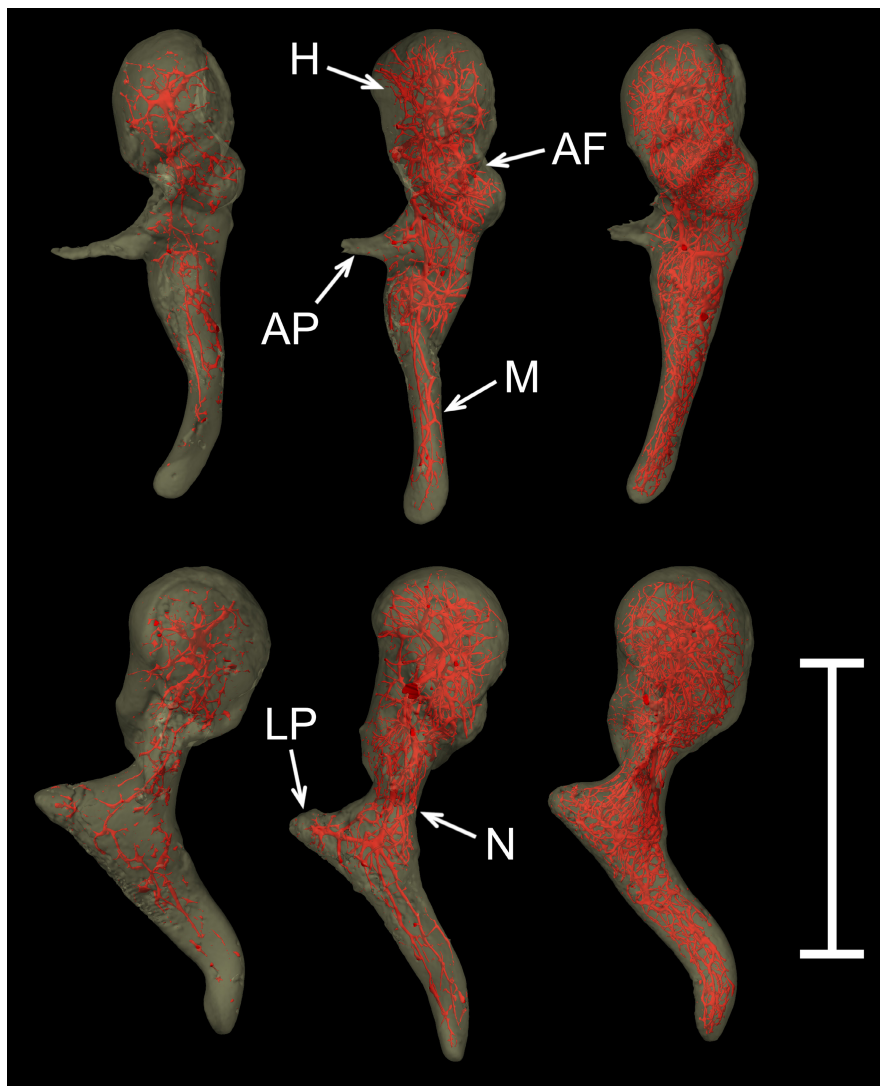


FIGURE 3 Reconstructions of three mallei, seen in medial view (upper row) and anterior view (lower row). The ossicular bone is shown translucent; internal vascular channels and cavities are shown in red. The specimen on the left has unusually sparse channels; the specimen on the right has unusually dense channels. The central specimen has a more typical channel density. AF, articulation facet; AP, anterior process; H, head; LP, lateral process; M, manubrium; N, neck. Scale bar = 5 mm

and narrowed to leave the distal third of the manubrium relatively undersupplied.

Many branches from the network of channels within the malleus reached the surface at tiny foramina, which were most commonly found scattered around the head, neck, lateral process and proximal manubrium. There were often several very small foramina on the facet for articulation with the incus. The anterior process was notably lacking in channels, the network within the main part of the ossicle penetrating only its base, and it was consistently free of foramina.

3.2 | Incus

As with the malleus head, the most radiodense bone of the incus body and short process tended to be peripheral, with less dense regions deeper within (Figure 2b). The long process and lenticular apophysis were very radiodense, even in specimens which had eroded long processes (see later).

The basic vascular architecture within the incus involved a large cavity within the central part of the head and body, larger than the equivalent in the head of the malleus. From here, a main channel extended posteriorly into the short process. Another main channel passed down through the long process to communicate with the exterior by means of a foramen within the hollowed region just dorsal to the pedicle supporting the lenticular apophysis (Figure 2b). The apophysis itself was consistently free of channels large enough to be identified as such.

The shape and size of the central cavity of the incus varied considerably among the 12 specimens examined, but it was typically broadest rostr dorsally, tapering towards the short process,

mediolaterally flattened and often lobed rather than simple in shape. Numerous channels radiated outwards from this cavity, their highest density remaining within the head and body, with a lower density around the periphery of the ossicle. There would always be multiple smaller channels running into the short and long processes in parallel with the main channel, and all these channels would branch and intercommunicate (Figure 4). The great majority of specimens conformed to the general pattern shown in Figure 2b. However, in three specimens, several channels of similar size extended into the short process such that it was impossible to identify one main channel. The main channel in the long process was disrupted by erosion in several specimens, but the sections remaining conformed to the general pattern. In one, there was too much erosion to tell; only in the specimen which had the unusually sparse channel structure were there several channels of similar width instead of one main channel within the long process (Figure 5).

Each incus had two to four main communicating channels, varying in position, which connected the central cavity/channel system to the exterior. In nine specimens, a medium-sized channel, arising at a foramen on the lateral side of the body near the articulation facet, travelled posteromedially to meet the central cavity. Six of these nine specimens also had a channel passing into the central cavity from a foramen in the middle of the body, on the medial side. Other positions where large communicating channels met the ossicular surface in particular specimens included the base of the long process ($n = 5$) and the articulation facet ($n = 1$). Smaller foramina were scattered around the surface of the incus, the highest density generally being on the body of the ossicle and proximal long process, medially. There were always fewer foramina on the lateral surface. One or more very small foramina were commonly found somewhere on the articulation facet ($n = 10$ specimens).

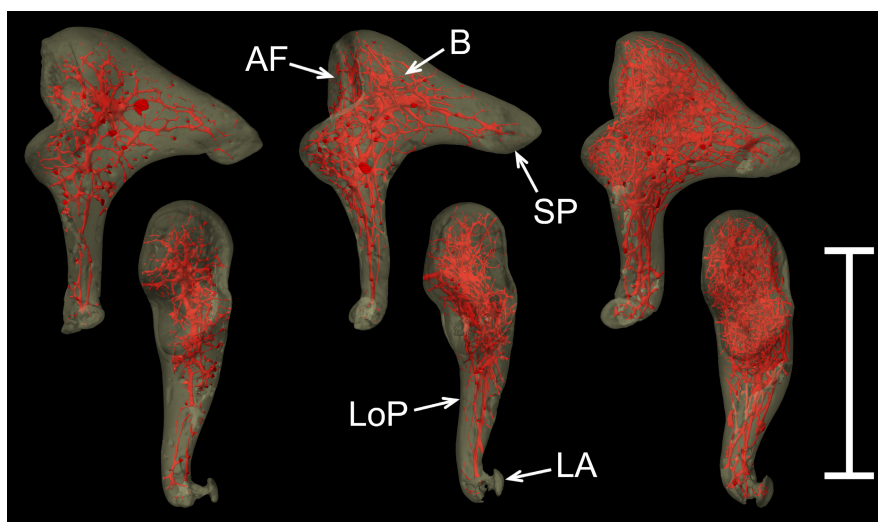


FIGURE 4 Reconstructions of three incuses, from the same three donors as the mallei shown in Figure 3, seen in medial view (upper row) and anterior view (lower row). The ossicular bone is shown translucent; internal vascular channels and cavities are shown in red. The specimen on the left has unusually sparse channels; the specimen on the right has unusually dense channels. The central specimen has a more typical channel density. AF, articulation facet; B, body; LA, lenticular apophysis; LoP, long process; SP, short process. Scale bar = 5 mm

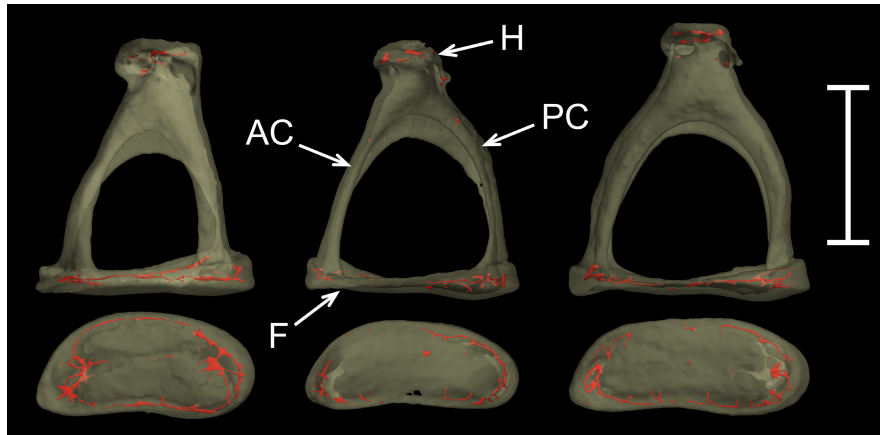


FIGURE 5 Reconstructions of three representative stapedes, dorsal view (upper row), and a view of their footplates from medially (lower row). The ossicular bone is shown translucent; internal vascular channels and cavities are shown in red. The resolution of the scans was not sufficient to reconstruct all the channels, but it appears that there is a ring of channels around the periphery of the footplate. AC, anterior crus; F, footplate; H, head; PC, posterior crus. Scale bar = 2 mm

3.3 | Stapes

The most radiodense bone in the stapes tended to be in the thicker regions of the head and footplate.

The channels in the stapes were very narrow and many did not meet the thresholding criterion for modelling. As a result, the reconstructions of the channel architecture of this ossicle were crude, precluding an accurate description. Channels were, however, always visible within the neck and head region, and within the footplate (Figure 3). The footplate, crura and neck of the human stapes are internally hollowed where they surround the intercrural foramen, such that these structures are U-shaped in cross-section. Some of the short channels that were found in the neck and head opened within the hollowed interior of the neck, while others opened onto the outside of the neck. The articular surface of the head was free of foramina. There were always one or more long and narrow channels extending around the perimeter of the footplate, within the bone, where the thick, outer labrum meets the thinner, central footplate. These perimeter channels were more obvious towards the poles, and seemed to be supplied by foramina located where the crura met the footplate, within the hollowed region of each crus. It was not clear whether the narrow channels extending from the anterior and posterior poles of the footplate around the perimeter met in the middle to form a complete ring, because the channels in the middle region were very narrow and poorly reconstructed. Between the neck and the footplate, the crura of the stapes appeared to be largely free of channels, although one or two short and narrow tubes were occasionally found penetrating all the way through the thin crural bone.

3.4 | Ossicular erosion

Many of the ossicular specimens examined in this study contained localised regions where the bony surfaces appeared roughened,

indented or more deeply excavated. The irregular appearance of these regions (Figure 1) suggested some kind of erosion.

The surface of the malleus tended to be relatively smooth except for the region just dorsal to the anterior process, which was always indented and roughened around where the main foramina were found. In the great majority of specimens, the surface of the manubrium was indented with shallow pits, many of which did not appear to be associated with the deeper channel structure. The extent of this pitting varied from occasional pock-marks to a wider excavation of part of the manubrial surface. There seemed to be no common pattern to the area affected, which could include proximal or distal parts of the process, or in some cases the whole manubrium. The tip of the lateral process was often affected in a different way, with multiple, very small indentations giving it a rough or spongy appearance in several mallei. These excavations to manubrium and lateral process were only ever superficial, and the channels running down the length of the manubrium were too deep to be affected. Elsewhere, localised patches of what seemed to be erosion of the ossicular surface were found only occasionally, on the neck, head or articulation facet of individual mallei. Like the indentations of the manubrium, these eroded regions were only ever superficial and did not seem to impact on the channel structure deeper within the ossicle.

The body and short process of the incus were in most cases relatively smooth except for the foramina, although some apparently eroded areas were found in some specimens on the head or articulation facet. The long process of the incus, however, showed some degree of erosion in all 12 specimens:

1. The long process was found to have only superficial erosion in one specimen, in its middle section.
2. In eight specimens, there was erosion at the distal end of the long process, around the base of the pedicle supporting the lenticular apophysis (Figure 6a). The apophysis itself appeared to be unaffected, although its connection to the long process could be quite tenuous. There was in most cases some erosion to the proximal or middle long process too, but there was no disruption to the main

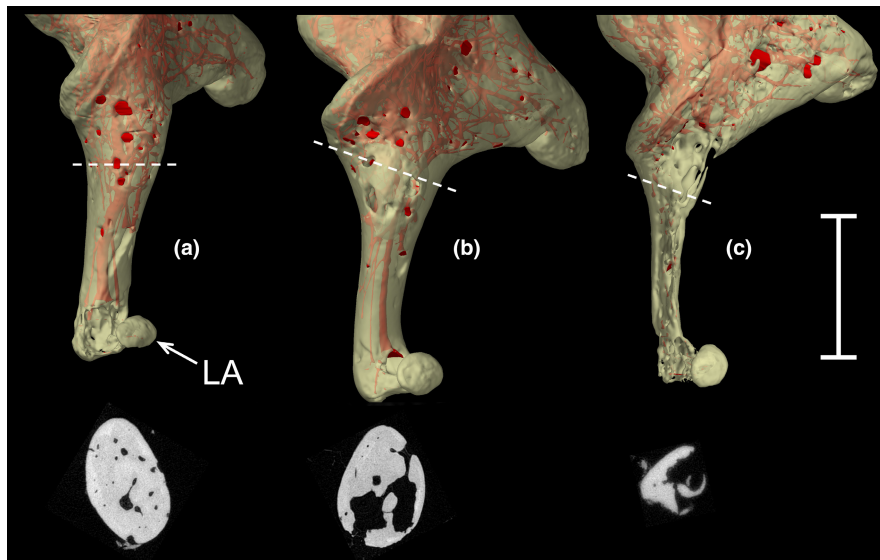


FIGURE 6 Reconstructions of three incudes, in anteromedial view, showing different states of erosion of their long processes. The ossicular bone is shown semi-transparent; internal vascular channels and cavities are shown in red. Tomogram cross sections, at the positions indicated by dotted lines, are presented below. Process (a) shows erosion around the distal long process near the lenticular apophysis (LA) only, but no disruption of the vascular channels running down the main part of the process. The proximal part of process (b) shows considerable internal erosion, with excavated cavities connected to the exterior through several large holes, but this is not obvious from an external view. Some of the vascular channels have been disrupted in this region, but others remain intact. Process (c) shows extreme erosion along its whole length: The bone remaining is very thin and all major vascular channels have been obliterated. Scale bar = 2 mm

vascular channels running down the process in four of these eight specimens.

3. In three specimens, erosion into the proximal or middle long process was deep enough to disrupt at least one of the main vascular channels running within it (Figure 6b). Channels would in some cases end abruptly when they reached an eroded region, while in other cases they seemed to expand and merge with the eroded cavities. However, the remaining bone was thick enough to contain other channels, which continued uninterrupted to the end of the process. The eroded cavities within the process were in communication with the exterior through relatively narrow openings resembling wide foramina. Because of this, these long processes, although hollowed out internally, seemed intact on superficial external inspection.
4. Four specimens had more extensive erosion of their long processes, to the point that all the significant vascular channels running down the length of the processes were either interrupted at some point or completely obliterated; only very small channels remained (Figure 6c). The eroded areas were in wide communication with the exterior, and obvious from external view. In the most extreme case, the erosion extended upwards into the body of the ossicle, on the posterolateral side.

The dorsal surface of the neck of the stapes appeared irregularly eroded to some extent in all specimens examined. This erosion varied from shallow cavities to major excavation of the whole dorsal neck region. In the more extreme cases, the excavation would communicate with the deep sulcus which extends into the neck from the intercrural foramen. The articular part of the head of the stapes always remained intact, however. The ventral side of the neck of the stapes was smooth and uneroded in most specimens; any erosion observed there was relatively minor.

3.5 | The notch in the incudal short process

In six of the 12 incudal specimens, there was a notch in the ventral side of the short process of the incus (Figure 2b). In a seventh specimen there was a circular pit in the same place. These notches were visible in the temporal bone scans that had been made prior to dissecting out the ossicles, so they were not a dissection artefact. In all cases, the notch or pit was filled with soft tissue. In all but two specimens, this soft tissue was clearly continuous with the ligamentous tissue connecting the short process to the posterior wall of the tympanic cavity. Unlike the large foramina on the body of the incus which were in wide communication with the channels and cavities within, the notch on the short process was not an inlet point for any major blood vessels. Only the occasional small channel opened into it, in some specimens.

One of the incudal specimens which lacked a notch instead had a small, irregularly shaped cavity within the same region of the short process, which did not communicate with the exterior. In the remaining four specimens there was no notch, pit or cavity within the short process. The medial side of the short process was flattened, to a greater or lesser extent, in these specimens.

3.6 | Ossicular masses and densities

The directly measured masses of the ossicles are presented in Table 1, together with the percentages of the total volumes occupied by channels and the ossicular densities. A coefficient of variation (C.V.) is the standard deviation (S.D.) divided by the mean, expressed as a percentage: a comparison of C.V. values shows that

TABLE 1 Measurements made from the ossicles ($n = 12$ specimens)

| | Mass, mg | | Percentage channels and cavities, by volume | | Density, mg mm^{-3} | |
|----------|----------|-------|---|-------|------------------------------|-------|
| | Malleus | Incus | Malleus | Incus | Malleus | Incus |
| Mean | 27.61 | 29.09 | 3.97 | 5.73 | 2.16 | 2.11 |
| S.D. | 2.79 | 3.36 | 1.53 | 2.11 | 0.03 | 0.04 |
| Min | 20.49 | 23.48 | 1.13 | 2.38 | 2.12 | 2.05 |
| Max | 30.32 | 33.67 | 6.29 | 9.74 | 2.21 | 2.17 |
| C.V. (%) | 10.11 | 11.56 | 38.45 | 36.81 | 1.41 | 1.83 |

Abbreviation: C.V., coefficient of variation.

the percentage of vascular channels and cavities by volume was relatively much more variable than the masses or densities of the ossicles.

Because measurements were available from the malleus and its cognate incus from each donor, we compared malleus and incus measurements using paired *t*-tests. We excluded one specimen in which part of the short process of the incus had been damaged during the dissection process. There were significant differences between malleus and incus masses ($p = 0.023$), percentage channels and cavities ($p = 0.008$) and ossicular densities ($p = 0.002$). Compared to their cognate incudes, nine out of 11 mallei had a lower percentage of channels and cavities, and 10 out of 11 mallei were more dense. The same trends applied to the malleus-incus pair excluded from the statistical analysis.

Using linear regression, no significant relationship was found between ossicular mass and the percentage volumes of the internal ossicular channels and cavities, for either mallei or incudes (Figure 7a). Overall, the ossicular density decreased as percentage of channels and cavities increased, and the relationship was significant for both mallei and incudes (Figure 7b). The slopes and intercepts of the two lines in Figure 7b were compared using the method given by Zar (1996). The slopes proved to be very similar indeed and no significant difference was found between them ($p = 0.859$), but a significant difference was found in the intercepts ($p = 0.013$). This is consistent with the finding described above, that malleus density is greater than incus density.

4 | DISCUSSION

Based on a careful comparison of 12 specimens, we established and illustrated the basic pattern of the main channels and cavities within the malleus and incus (Figure 2). These findings are broadly consistent with the scattered observations found in the literature (e.g. Anson & Winch, 1974; Enghag et al., 2019; Kirikae, 1960; Nager & Nager, 1953). Superimposed on this basic structure, however, is a very complex, intercommunicating network of vessels which varies considerably between individuals, obscuring the basic pattern. Data in Table 1 show that the percentage by volume of vascular channels and cavities within the malleus and incus can vary 4- to 5-fold between different individuals. The ossicles with the highest percentage volumes of channels and cavities were those with relatively large central cavities; the surrounding network of blood vessels seemed to

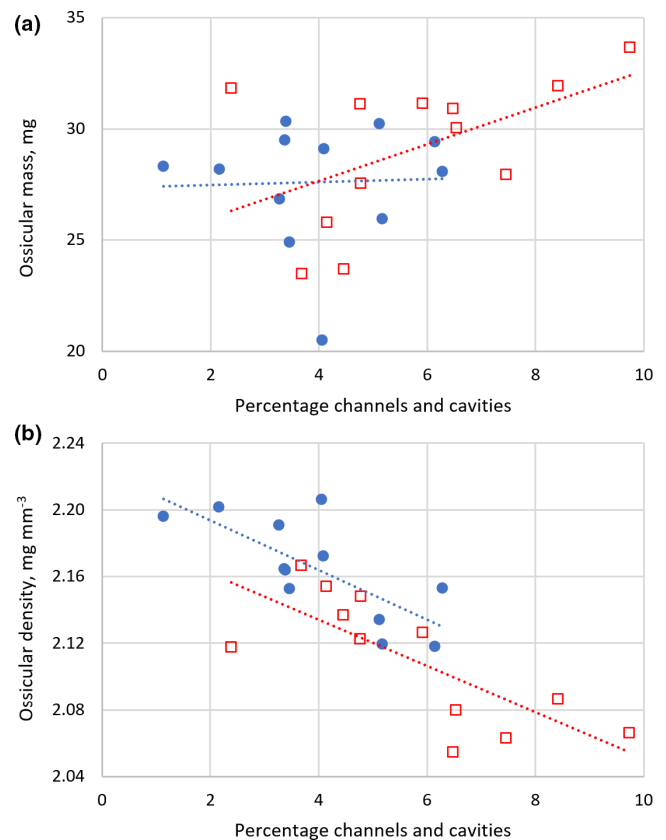


FIGURE 7 The relationships between (a) ossicular mass and percentage volume of internal vascular channels and cavities, and (b) ossicular density and percentage volume of internal vascular channels and cavities, in 12 mallei (solid, blue circles) and 12 incudes (open, red squares). Least-squares regression lines have been fitted to malleus and incus data separately. In (a), for the malleus regression $R^2 = 0.001$, $p = 0.910$; for the incus regression, $R^2 = 0.270$, $p = 0.084$. In (b), for the malleus regression $R^2 = 0.552$, $p = 0.006$; for the incus regression, $R^2 = 0.569$, $p = 0.005$

contribute less. The extent of the individual variation is obvious from the reconstructions in Figures 3 and 4.

4.1 | Contents of ossicular channels and cavities

The ossicles examined were dry at the point of scanning, which is why some of the larger channels and cavities were air-filled. Smaller

ones tended to be filled with low-radiodensity material which was presumably dried soft tissue, the nature of which could not be ascertained from the tomograms. However, there have been many histological studies of the ossicles featuring photomicrographs which show that these channels contain blood vessels (Anson et al., 1964; Anson & Winch, 1974; Hamberger & Wersäll, 1964; Lindeman, 1964; Nager & Nager, 1953; Pollock, 1959). Some of the smaller and more peripheral vascular channels might represent Haversian canals, which have been found at a particularly high density around the malleoincudal articulation (Kirikae, 1960). Anson and Winch (1974) found that the larger ossicular channels often contain two or more vessels. A photomicrograph in Nager and Nager (1953) shows what appears to be one of the wider cavities within the body of the incus, identified by those authors as a 'marrow space', within which can be seen a network of smaller vessels cut in cross-section. Pollock (1959) describes, in normal mallei and incudes, 'marrow spaces' containing a 'network of fine connective tissue which supports a network of capillaries'. These studies suggest that the large cavities within the malleus and incus, as reconstructed in the present work, do not each represent one expanded vessel or sinus. Instead, these spaces contain several smaller vessels, which presumably divide to form the branches which radiate away from those cavities, as well as non-vascular connective tissue. Yokoyama et al. (1999) found that the true bone marrow spaces within the malleus and incus get smaller as the ossicles grow, becoming converted to vascular channels by the age of 25 months.

Bradel et al. (2017) did not find any large vascular cavities within the ossicles of the single specimen they examined by serial grinding, but did identify one very small region within the head of the malleus, and several larger regions within the body and short process of the incus, which were said to be cartilaginous. Cartilage within the internal structure of adult ossicles has rarely been mentioned in the literature, but small islands of cartilage, representing embryonic remnants, were described by Oesterle (1933). These were mainly found around the periphery of the ossicles, between the periosteal and endochondral regions, especially in the manubrium and lateral process of the malleus, the short process of the incus, and around the stapes footplate. It is possible that some of the 'vascular' cavities in our reconstructions actually contained some cartilage too, although Oesterle's description of where the cartilage remnants tend to be found does not coincide with the more central location of the larger cavities we found in our ossicles. Our reconstructions of the ramifying pattern of channels and cavities are, however, strikingly similar to the pattern of blood vessels visible in the cleared malleus and incus specimens shown by Kirikae (1960), and the positions of the main axial channels of the ossicles that we show in Figure 2 are close to the positions of the main channels sketched by that author. This supports our contention that these channels and cavities are indeed vascular in nature.

While we believe that our reconstructions accurately represent the main vascular channels of the mallei and incudes, we cannot say the same of our stapes reconstructions. All channels in the stapedes

were very small, and the resolution of our scans was insufficient to reconstruct even the larger ones satisfactorily. In order to visualise these tiny channels properly, a more advanced technique such as synchrotron-based X-ray phase contrast imaging is necessary. Using this technique, Anschuetz et al. (2019) were able to observe a channel passing from the head of the stapes down through the posterior crus to reach the footplate. We were able to confirm that vessels penetrate the neck and head of the stapes, but we did not find any vessels passing along the length of the crura within the bone. Although Hamberger and Wersäll (1964) did not believe that vascular channels are normally present in the footplate, we identified channels within the bony rim of the footplate in every specimen examined, as described in several histological papers (Anson et al., 1964; Anson & Winch, 1974; Nager & Nager, 1953). Lindeman (1964) found the blood vessels within the stapes footplate to be particularly prominent anteriorly and posteriorly, at the junctions of crura and footplate, and this is where they were largest and most consistently reconstructed in our study too. Curiously, Anschuetz et al. (2019) refer to a vascular ring along the annular ligament of the stapes footplate, but do not refer to channels within the bone of the footplate itself.

4.2 | Ossicular foramina

The malleus and incus were found to have multiple foramina of different sizes scattered over their surfaces, except for some particular areas such as the anterior process of the malleus, which was very poorly vascularised, and the lenticular apophysis of the incus. Incudal foramina were present at a higher density on the medial side than on the lateral side, as noted by Lindeman (1964). Although the positions of the largest foramina leading to the central channels of the ossicles varied between individuals, there is broad agreement in the literature on where these tend to be located (Table 2). However, Gerlinger et al. (2009), using light microscopy, identified 'nutritive foramina' on the long processes of 52 out of 100 incudes from 50 donors of mean age 69 years, but none on the bodies of any of their ossicles. It seems possible that some of what Gerlinger et al. had identified as nutritive foramina in fact represented excavated regions of the long processes of some of their specimens, and that the nutrient foramina on the ossicular bodies had been overlooked.

4.3 | Ossicular erosion

All 12 incudal specimens examined in this study showed some degree of erosion to the long process of the incus. In some cases this could be very extreme, such that four specimens had no significant channels running uninterrupted from the body of the incus down to the distal tip of the process. There was no clear link between the extent of erosion observed in the ossicles and the age or sex of the donors, but it should be noted that the youngest donor was 70. Medical histories of the cadaveric donors were not available and no tympanic

TABLE 2 Recorded positions of the major foramina on the surfaces of the ossicles

| Paper | Malleus | Incus | Stapes |
|-------------------------|--|--|---|
| Nager and Nager (1953) | <ul style="list-style-type: none"> • Anterolateral neck or lower part of head | <ul style="list-style-type: none"> • Lateral side of body (most common) • Medial side of body near joint capsule • Anterolateral surface of root of long process • Lower end of long process | <ul style="list-style-type: none"> • Neck and head • Base of anterior crus near footplate • Posterior part of thickened rim of footplate |
| Kirikae (1960) | <ul style="list-style-type: none"> • Anterolateral neck • Lower part of head near lateral malleolar ligament | <ul style="list-style-type: none"> • Medial aspect of body near articulation • Anterolateral surface of root of long process | |
| Hamberger et al. (1963) | <ul style="list-style-type: none"> • Head of the malleus • Lateral aspect of malleus neck (1 or 2 foramina) | <ul style="list-style-type: none"> • Superior part of body near articulation with malleus • Base of short process • Base of long process | <ul style="list-style-type: none"> • Lower side of head |
| Gerlinger et al. (2009) | | <ul style="list-style-type: none"> • Anteromedially on proximal and middle thirds of long process • (no foramina observed on body) | |
| Bradel et al. (2017) | <ul style="list-style-type: none"> • Lateral side of neck (two foramina) • Medial side of neck | <ul style="list-style-type: none"> • Lateral side of body, near base of long process and close to articulation • Medial side, base of long process • Medial side, base of short process | <ul style="list-style-type: none"> • Anterior surface of head |
| Anschuetz et al. (2019) | <ul style="list-style-type: none"> • Anterior surface of head • Neck | <ul style="list-style-type: none"> • Lateral side of body, near base of long process and close to articulation • Medial side, base of long process • Medial side, base of short process | <ul style="list-style-type: none"> • Anterior surface of head |
| Enghag et al. (2019) | | <ul style="list-style-type: none"> • Lateral side of body, near articulation • Proximal long process • Distal long process near pedicle • Medial surface of incudal body | |
| Present study | <ul style="list-style-type: none"> • Anterior head, just dorsal to anterior process (one or two foramina) | <ul style="list-style-type: none"> • Lateral body, close to articulation facet ($n = 9$) • Medial body, centrally ($n = 6$) • Proximal long process ($n = 5$) | <ul style="list-style-type: none"> • Within hollowed part of neck • Outside of neck • Within hollow region of crura, where they meet footplate |

membrane retraction was visible in the temporal bone scans, prior to dissection, so the possible causes of this erosion remain unknown.

Erosion of the long process of the incus has been well documented in the literature. Anson and Bast (1959) show histological sections of substantially eroded incudal long processes in infants as well as adults, together with evidence of repair through new bone deposition. Using scanning electron microscopy, pitting characteristic of osteoclastic bone erosion has been found on the distal long process and on the lenticular apophysis of normal incudes, there being progressive levels of erosion with age (Lannigan et al., 1993a; Lannigan et al., 1995). Chen et al. (2008) found that the long process was deeply pitted, some of the pits eroding the bone around the vascular foramina. In several of our specimens, excavated regions inside the proximal long process were found to be in communication with the exterior through holes resembling large foramina (Figure 6b), which would be consistent with the erosion beginning around true vascular foramina and extending inwards. Duboeuf et al. (2015) found cavities containing fibrocellular tissue and adipocytes within human incudes from patients who had suffered chronic middle ear inflammatory diseases. It is possible that the eroded, air-filled spaces identified in some of the ossicles examined in the present study had similarly been filled with soft tissue in vivo, which had subsequently dried.

The notch observed in the short processes of six out of 12 incudes (Figure 2b) was apparently not part of the vascular channel structure. It was filled with soft tissue which, in four cases, was continuous with the posterior incudal ligament. This notch has been previously recorded in around 40% of human incudes, including in neonates (Arensburg & Nathan, 1971; Unur et al., 2002). The notch appeared smooth-walled and in a consistent position. Together with its recorded presence in neonates, this suggests that it is not a result of pathological erosion. The presence or absence of a notch on the short process of the incus was not obviously linked to age or sex.

The dorsal neck of the stapes was consistently found to be eroded in the present study. The mallei were less affected by erosion, although the bony surface just dorsal to the anterior process was always roughened and there was usually some pitting on the manubrium. Chen et al. (2008) also found eroded areas around the stapes neck, but the mallei they examined were largely unaffected. Vallejo-Valdezate et al. (2016) interpreted the pitting they observed on the manubrium through scanning electron microscopy as representing the openings of vascular channels, which would in life contain blood vessels penetrating the manubrium from the tympanic region. In the present study, only some of the manubrial pits seemed to lead to the internal vascular channels. It may be that some

of the pitting of the manubrium might in fact be in regions of bone which would be covered with a layer of cartilage *in vivo*; several studies have identified cartilage enveloping the human manubrium, even in adult specimens (Anson et al., 1964; Anson & Winch, 1974; Oesterle, 1933). The roughened appearance of the lateral process in some of our specimens might similarly relate to the presence *in vivo* of a 'cap' of cartilage (Michaelides et al., 2018).

4.4 | Clinical relevance of the internal ossicular blood supply

Because the vessels of the distal long process of the incus are subjected to surgical damage, there has been particular interest in the blood supply to this part of the ossicular chain (Alicandri-Ciuffelli et al., 2018; Lannigan et al., 1993b). Its dual supply comprises both external mucosal and internal vessels.

Although there is considerable variability between individuals, Alberti (1963) noted that just one blood vessel commonly reaches the end of the long process via an internal channel, whereupon branches often exit the bone near the tip of the process to anastomose with a mucosal vascular network. We found that there were typically several parallel channels within the long process, but one main channel among these would reach the exterior in the hollowed region just dorsal to the pedicle supporting the lenticular apophysis. This was also described by Enghag et al. (2019), who referred to this hollowed region as the 'anterior concavity'. It seems likely that blood vessels would communicate here with the mucosal vessels around the incudo-stapedial articulation. As described by Alberti (1963), this mucosal network is formed from vessels running down the surface of the long process and vessels running over the stapes or stapedius tendon. The lenticular apophysis of the incus is supplied by this mucosal network, and/or an internal supply coming directly from the vessel(s) within the long process.

Historically, necrosis of the long process of the incus was sometimes observed when the stapes was replaced by a prosthesis attached to the long process (Alberti, 1965), a procedure which might be performed in an attempt to correct conductive hearing loss in conditions such as otosclerosis. Tight fixation of the prosthesis to the long process is likely to obstruct mucosal vessels, in which case the incudal bone may become more dependent on its internal vascular network. In our specimens, erosion of the proximal long process was often significant enough to disrupt the passage of one or more vascular channels. It would be easy to overlook the early stages of this kind of damage, especially if there is substantial internal erosion without very obvious exterior damage (Figure 6b), a condition which Oesterle (1933) also briefly noted. We could not tell from our CT scans whether vessels might still run through the eroded spaces, no longer enclosed within their normal bony canals. However, it is important for clinicians to be alert to the possibility that the internal ossicular vessels may well be progressively disrupted during the process of erosion. If so, damage to the mucosal vessels through application of a prosthesis could be associated with a greatly increased

risk of necrosis. Modern techniques use thermo-responsive alloys, which form a tight, circumferential fixation of the prosthesis to the long process, and these new prostheses are not associated with a high incidence of long process necrosis. However, erosion of the long process is commonly observed when stapedectomy or stapedotomy surgeries fail post-operatively (Lesinski, 2002).

Erosion of the long process of the incus has also been observed following pars tensa retraction (Kasbekar et al., 2014) and cholesteatoma (Maresh et al., 2011; Mohammadi et al., 2012). This process involves remodelling of the long process with loss of a distinct lenticular pedicle: we did not encounter pathologies of this nature in our series. The widespread use of a fibre-guided laser to vaporise the lesion during cholesteatoma removal procedures does not typically cause necrosis of the malleus or incus, including the healthy incudal long process (Hamilton, 2014). Laser energy is tolerated less well by the stapes crura, the lenticular pedicle and eroded incudal long processes, all regions which we have found to have poor internal blood supplies. We suggest that the normal resistance of ossicular bone to necrosis following such procedures is due to its internal vasculature; those areas with a limited internal supply either normally or pathologically are less robust after surgical disruption of their external supply.

Cholesteatoma and pars tensa retraction are more often observed within a younger age-range than the donors included in this study, and surgery for otosclerosis is infrequently performed on patients of advanced age. Further investigation into ossicular microvasculature in younger specimens would help us to understand whether elderly patients are more likely than younger ones to have a reduced internal blood supply to their ossicles, which would put them more at risk of ossicular necrosis.

4.5 | Ossicular volumes, masses and densities

To make our reconstructions as comparable as possible, all of our ossicles were scanned using the same settings, and we used the same greyscale thresholds to separate 'bone' from 'non-bone'. There was an element of subjectivity involved in placing the outer boundaries where channels and cavities were continuous with the external environment. This was especially problematic in eroded regions of bone where these boundaries were not on the normal outer surface of the ossicles. Even so, errors in placing boundaries in these limited regions within the thin processes are very unlikely to have any significant impact on the volumes of the channels and cavities measured from the ossicles as a whole. The effect of ignoring the very narrowest channels, which failed to meet our threshold for identification of 'non-bone', is likely to be trivial, given that these channels were so tiny.

Any soft tissue within our ossicles would have been dry at the point of weighing: many of the larger internal cavities and channels were seen in the scans to be air-filled. However, any reduction in mass from drying of the internal cavities would have been offset by the presence of residual soft tissue clinging to the surface of the ossicles. The mean

masses for malleus and incus (Table 1) measured here were close to some values in the literature (Nummela, 1995; Sim & Puria, 2008); the mean values presented by Kirikae (1960) and Chen et al. (2008), presumably taken from Japanese cadavers, were a little lighter.

Mean ossicular densities calculated by Sim and Puria (2008) were 2.31 mg mm^{-3} for the human malleus and 2.14 mg mm^{-3} for the incus ($n = 4$ each). This malleus density is higher than any value we calculated, although the incus density is close to our mean (Table 1). However, Sim & Puria assumed that the ossicular mass they weighed was entirely 'bone', and computed densities on the assumption that the density of the vascular spaces within their ossicles in vivo would be 1.00 mg mm^{-3} . Making the same assumption with our data, and excluding the specimen with a damaged incus, raises our mean density values (malleus 2.20 mg mm^{-3} , incus 2.17 mg mm^{-3} , $n = 11$ each), but only a little because the channels and cavities occupy such a small proportion of ossicular volume in most specimens (Table 1). The density difference between malleus and incus remains significant (paired t -test; $p = 0.004$).

In order to compute the density of the bony component only of the ossicles, that is excluding the channels and cavities, we need to make an assumption about what was in those channels and cavities at the point of weighing. If we assume, like Sim and Puria (2008), that the masses we measured were of the 'bone' component only, that is all channels and cavities were completely empty, we calculate densities of 2.26 and 2.24 mg mm^{-3} for malleus and incus bone respectively ($n = 11$ each): the difference is not significant ($p = 0.108$). A p value below 0.05 would be found, however, if we assumed that the channels had been 20% or more filled with dried soft tissue (density 1.00 mg mm^{-3}) on weighing. If completely filled with soft tissue, mean bone density would take the lowest possible values of 2.21 mg mm^{-3} for the malleus and 2.18 mg mm^{-3} for the incus ($p = 0.005$). Whatever assumption we make, differences between malleus and incus bone density are clearly very small, and the comparisons are vulnerable to error based on different relative amounts of residual soft tissue clinging to the exterior of the mallei and incudes. There is, however, an indication that malleus bone may, on average, be slightly more dense than incus bone. This would be consistent with the relative proportions of the higher- and lower-radiodensity bone visible in the two ossicles (Figure 2).

Our measurements and calculations lead us to conclude that:

1. Mean incudal mass is slightly higher than mean malleus mass. This has often been found to be the case in previous studies (see e.g. Chen et al., 2008; Kirikae, 1960; Nummela, 1995; Sim & Puria, 2008);
2. Mean malleus density is higher than mean incus density;
3. This higher malleus density is mainly due to a lower proportion of channels and cavities within it, compared to the incus. The osseous component of the malleus may also be of very slightly higher density than that of the incus.

ACKNOWLEDGEMENTS

The authors thank Prabhvir Marway, Will Ashley-Fenn, Darren Broadhurst and Maria Wright for initial preparation of the temporal

bone specimens that we used, and Cecilia Brassett and Richard Lloyd for their essential help with project logistics and permissions. Graham Treece and Andrew Gee generously advised on the use of the reconstruction software Stradview, which they had created. Finally, we thank the two reviewers of this manuscript for their constructive comments.

AUTHOR CONTRIBUTIONS

MJM conceived the project, made the CT scans, contributed to the reconstructions and led the production of the draft manuscript. SMM performed the dissections and worked on the reconstructions. RG and JH provided essential clinical insight. All four authors participated in the interpretation of data and writing of the paper.

DATA AVAILABILITY STATEMENT

The CT data that support the findings of this study are available on request from the corresponding author. The data are not publicly available due to privacy and ethical restrictions.

ORCID

Matthew J. Mason  <https://orcid.org/0000-0001-7845-0720>

REFERENCES

- Alberti, P.W. (1963) The blood supply of the incudostapedial joint and the lenticular process. *Laryngoscope*, 73, 605–628.
- Alberti, P.W. (1965) The blood supply of the long process of the incus and the head and neck of stapes. *Journal of Laryngology and Otology*, 79, 964–970.
- Alicandri-Ciuffelli, M., Guarino, P., Fabbri, F., Cunsolo, E.M., Presutti, L. & Anschuetz, L. (2018) Middle ear microvascularization: an "in vivo" endoscopic anatomical study. *European Archives of Oto-Rhino-Laryngology*, 275, 889–894.
- Anschuetz, L., Demattè, M., Pica, A., Wimmer, W., Caversaccio, M. & Bonnin, A. (2019) Synchrotron radiation imaging revealing the sub-micron structure of the auditory ossicles. *Hearing Research*, 383, 107806.
- Anson, B.J. & Bast, T.H. (1959) Development of the incus of the human ear; illustrated in atlas series. *Quarterly Bulletin of Northwestern University Medical School*, 33, 110–119.
- Anson, B.J., Harper, D.G. & Winch, T.R. (1964) Intra-osseous blood supply of the auditory ossicles in man. *Annals of Otology, Rhinology and Laryngology*, 73, 645–658.
- Anson, B.J. & Winch, T.R. (1974) Vascular channels in the auditory ossicles in man. *Annals of Otology, Rhinology and Laryngology*, 83, 142–158.
- Arensburg, B. & Nathan, H. (1971) Observations on a notch in the short (superior or posterior) process of the incus. *Acta Anatomica*, 78, 84–90.
- Bradel, S., Doniga-Crivat, L., Besdo, S., Lexow, F., Fehr, M., Lenarz, T. et al. (2017) Innovative 3D model of the human middle ear in high resolution with a histological microgrinding method: a feasibility study and comparison with μ CT. *International Journal of Otolaryngology*, 2017, 1–9. <https://doi.org/10.1155/2017/6753604>
- Chen, H., Okumura, T., Emura, S. & Shoumura, S. (2008) Scanning electron microscopic study of the human auditory ossicles. *Annals of Anatomy*, 190, 53–58.
- Duboeuf, F., Burt-Pichat, B., Farlay, D., Suy, P., Truy, E. & Boivin, G. (2015) Bone quality and biomechanical function: a lesson from human ossicles. *Bone*, 73, 105–110.
- Enghag, S., Strömbäck, K., Li, H., Rohani, S.A., Ladak, H.M., Rask-Andersen, H. et al. (2019) Incus necrosis and blood supply: a

- micro-CT and synchrotron imaging study. *Otology & Neurotology*, 40, e713–e722.
- Gerlinger, I., Tóth, M., Lujber, L., Szanyi, I., Móricz, P., Somogyvári, K. et al. (2009) Necrosis of the long process of the incus following stapes surgery: new anatomical observations. *Laryngoscope*, 119, 721–726.
- Hamberger, C.-A. & Wersäll, J. (1964) Vascular supply of the tympanic membrane and the ossicular chain. *Acta Oto-Laryngologica*, 57(suppl), 188.
- Hamberger, C.A., Marcuson, G. & Wersäll, J. (1963) Blood vessels of the ossicular chain. *Acta Oto-Laryngologica*, 56(183), 66–70.
- Hamilton, J. (2014) Functional orthogonal cholesteatoma surgery. In: Oswal, V. & Remacle, M. (Eds.) *Principles and practice of lasers in otorhinolaryngology and head and neck surgery*, 2nd edition. Amsterdam: Kugler Publications.
- Hemilä, S., Nummela, S. & Reuter, T. (1995) What middle ear parameters tell about impedance matching and high frequency hearing. *Hearing Research*, 85, 31–44.
- Homma, K., Du, Y., Shimizu, Y. & Puria, S. (2009) Ossicular resonance modes of the human middle ear for bone and air conduction. *Journal of the Acoustical Society of America*, 125, 968–979.
- Kasbekar, A.V., Patel, V., Rubasinghe, M. & Srinivasan, V. (2014) The surgical management of tympanic membrane retraction pockets using cartilage tympanoplasty. *Indian Journal of Otolaryngology and Head & Neck Surgery*, 66, 449–454.
- Kirikae, I. (1960) *The structure and function of the middle ear*. Tokyo: The University of Tokyo Press.
- Lannigan, F.J., O'Higgins, P. & McPhie, P. (1993a) Remodelling of the normal incus. *Clinical Otolaryngology and Allied Sciences*, 18, 155–160.
- Lannigan, F.J., O'Higgins, P. & McPhie, P. (1993b) The vascular supply of the lenticular and long processes of the incus. *Clinical Otolaryngology and Allied Sciences*, 18, 387–389.
- Lannigan, F.J., O'Higgins, P., Oxnard, C.E. & McPhie, P. (1995) Age-related bone resorption in the normal incus: a case of maladaptive remodelling? *Journal of Anatomy*, 186, 651–655.
- Lesinski, S.G. (2002) Causes of conductive hearing loss after stapedectomy or stapedotomy: a prospective study of 279 consecutive surgical revisions. *Otology & Neurotology*, 23, 281–288.
- Lindeman, H. (1964) Some histological examinations of the incus and stapes with especial regard to their vascularization. *Acta Oto-Laryngologica*, 57(188), 319–326.
- Maresh, A., Martins, O.F., Victor, J.D. & Selesnick, S.H. (2011) Using surgical observations of ossicular erosion patterns to characterize cholesteatoma growth. *Otology & Neurotology*, 32, 1239–1242.
- Michaelides, E., Kansal, A., Rutter, S. & Schutt, C. (2018) The malleus cap: anatomic description of cartilage of the lateral process of the malleus. *American Journal of Otolaryngology*, 39, 208–211.
- Mohammadi, G., Naderpour, M. & Mousaviagdas, M. (2012) Ossicular erosion in patients requiring surgery for cholesteatoma. *Iranian Journal of Otorhinolaryngology*, 24, 125–128.
- Nager, G.T. & Nager, M. (1953) The arteries of the human middle ear, with particular regard to the blood supply of the auditory ossicles. *Annals of Otology, Rhinology and Laryngology*, 62, 923–949.
- Nummela, S. (1995) Scaling of the mammalian middle ear. *Hearing Research*, 85, 18–30.
- Oesterle, F. (1933) Über den Feinbau der Gehörknöchelchen und seine Entstehung. *Archiv für Ohren-, Nasen- und Kehlkopfheilkunde*, 135, 311–327.
- Pollock, F.J. (1959) Pathology of ossicles in chronic otitis media. *AMA Archives of Otolaryngology*, 70, 421–435.
- Sim, J.H. & Puria, S. (2008) Soft tissue morphometry of the malleus-incus complex from micro-CT imaging. *Journal of the Association for Research in Otolaryngology*, 9, 5–21.
- Sim, J.H., Puria, S. & Steele, C.R. (2007) Calculation of inertial properties of the malleus-incus complex from micro-CT imaging. *Journal of Mechanics of Materials and Structures*, 2, 1515–1524.
- Unur, E., Ülger, H. & Ekinci, N. (2002) Morphometrical and morphological variations of middle ear ossicles in the newborn. *Erciyes Medical Journal*, 24, 57–63.
- Vallejo-Valdezate, L.A., Herrero-Calvo, D. & Garrosa-García, M. (2016) Vascularization of the long process of the malleus: surgical implications. *European Archives of Otorhinolaryngology*, 273, 2335–2342.
- Yokoyama, T., Iino, Y., Kakizaki, K. & Murakami, Y. (1999) Human temporal bone study on the postnatal ossification process of auditory ossicles. *The Laryngoscope*, 109, 927–930.
- Zar, J.H. (1996) *Biostatistical analysis*. London: Prentice Hall International (UK) Ltd.
- Zhou, L., Shen, N., Feng, M., Liu, H., Duan, M. & Huang, X. (2019) Study of age-related changes in middle ear transfer function. *Computational Methods in Biomechanics and Biomedical Engineering*, 22, 1093–1102.

How to cite this article: Manoharan, S.M., Gray, R., Hamilton, J. & Mason, M.J. (2022) Internal vascular channel architecture in human auditory ossicles. *Journal of Anatomy*, 241, 245–258. Available from: <https://doi.org/10.1111/joa.13661>